(Received 18 February 2025, Accepted 8 April 2025, Scheduled 6 May 2025)

Arbitrary Shape Transmitting Coils Optimization for One-to-Many Free-Positioning Wireless Power Transfer Systems

Pavel Smirnov, Aleksandr Miroshnikov, and Polina Kapitanova*

School of Physics and Engineering, ITMO University, Saint-Petersburg, Russia

ABSTRACT: Nowadays, misalignment tolerant wireless power transfer systems providing simultaneous power supply to several devices are the subject of intensive research in the field of wireless charging of electronic devices. A critical parameter in such systems is the uniformity of magnetic field generated by a transmitting coil. In this paper, we examine the characteristics of the magnetic field distribution of arbitrary shape planar transmitting coils and propose a genetic algorithm for optimizing their design with the objective of increasing the field uniformity. This study stands out from existing literature by introducing an optimization approach that not only encompasses traditional circular and square coils but also extends to convex polygonal coils. The results of the algorithm are validated experimentally on coils of three various geometries including circular, square, and hexagonal coils. The coefficient of variation of the magnetic field, which serves as a quantitative measure of its uniformity, is found to be 3.6% for the circular coil, 5.2% for the square one, and 5.1% for the hexagonal one in a region of interest encompassing half of the total area of the transmitting coil.

1. INTRODUCTION

Wireless power transfer (WPT) with magnetic coupling is a widely used method for powering various electronic devices [1]. It has found applications in areas such as consumer electronics [2], medical equipment [3], industrial machinery [4], electric vehicles [5, 6], smart home devices [7], and others. The primary reasons for the popularity of this technology and its active replacement of traditional wired power methods are increased user convenience and reliability as it eliminates the need for contact connections between the charged device and power sources.

The rapid growth in the number of electronic devices utilizing wireless charging has shifted the focus from WPT systems for charging a single receiver (Rx) from a single transmitter (Tx), which have been the most developed type, to charging of multiple Rxs simultaneously from a single Tx. While one-to-one WPT systems offer high power transfer efficiency, they come with limitations regarding user convenience and usage scenarios, as each Rx requires its own Tx. In contrast, one-to-many WPT systems allow for several Rxs to be powered simultaneously by a single Tx, making them more convenient and economically advantageous in many situations. Although the significant size asymmetry between the Rxs and Tx can lead to a decrease in the coupling coefficient and lower individual power transfer efficiency than one-to-one WPT systems, the overall efficiency, calculated as the sum of partial efficiencies, can still be sufficiently high and comparable to that of single-Rx systems.

To develop a one-to-many WPT system with free-positioning receivers, a uniform magnetic field distribution of a transmitting coil has to be achieved to ensure an equal power transfer efficiency to the receivers. To date, two main approaches have been proposed to provide a uniform distribution of a transmitting coil magnetic field. The first one utilizes arrays of coils to create a uniform magnetic field over the surface of transmitter. Thus, a single-layer array of properly positioned non-overlapping coils has been proposed in [8]. Later, additional coils have been introduced to an array of coils for field irregularities compensation [9]. Multi-layer overlapping coil arrays have also been employed wherein the coils are arranged in such a way that their total fields are uniform over the transmitting area [10]. One of the major advantages of this approach is the ability to achieve high power transfer efficiency by tracking receivers position and selective excitation of transmitting coils in the array that are closest to the receiver. However, the disadvantage of this approach is a complex and costly control system, which may not always be economically justified.

On the other hand, sole transmitting coils with optimized structure have been proposed and studied, which can be classified as a second approach for achieving uniform magnetic field, for instance, through the application of hybrid structures comprising concentrated winding and spiral winding designs [11], or the use of auxiliary coils for compensating of field irregularities [12]. Guided by the dependence of the magnetic field produced by a spiral coil on its dimensions, winding configurations, current magnitude, and winding directions, several different coil designs with nonuniform winding distributions have been proposed and investigated [13–15], with antiparallel current directions in individual coil windings [16] and varying current amplitudes in the windings [17, 18]. These studies have shown that achieving a uniform magnetic field distribution in a general manner is highly challenging, as it necessitates consideration of multiple factors like size and shape of the transmit-

* Corresponding author: Polina Kapitanova (p.kapitanova@metalab.ifmo.ru).

ting coil, size of the charging area, and the separation distance between the Rx and Tx. Consequently, there has been a rise in works employing genetic algorithm (GA) for the synthesis and optimization of planar spiral coils for one-to-many WPT systems [19–22], which offer relatively uniform magnetic field distributions with a relatively simple transmitting coil geometry.

While several optimization algorithms for planar spiral coils have been proposed, they mainly focus on standard shapes like circular and rectangular ones, which may not always be suitable for specific applications. As shown in [23], in the next-generation WPT systems, coil winding should be arranged in irregular shapes to maximize aperture sizes and mutual coupling. In this study, we propose a universal algorithm for optimizing the magnetic field distribution of transmitting coils for one-to-many WPT systems aimed to enhance the magnetic field uniformity. The algorithm's versatility stems from its ability to calculate and optimize magnetic fields for both standard-shaped transmitting coils and convex polygonal coils, which is beneficial for developing WPT coils that must fit within various device housings, maximizing the available area and system efficiency. This article outlines the methodology of the study, detailing the equivalent model of spiral coils and the apparatus used for calculating the magnetic field across various coil geometries. It introduces a quantitative parameter for estimating field uniformity and discusses the GA employed for coil optimization. An analysis of magnetic field distributions is provided for both a single current-carrying loop and a classic equidistant spiral coil, along with the results of the optimization and their experimental verification. Additionally, the article compares these results with existing literature and addresses potential challenges in generating uniform fields in large-sized coils.

2. METHODOLOGY

2.1. Magnetic Field Calculation

For an analytical description of a transmitting coil magnetic field, the method of multi-turn approximation can be employed [20]. The essence of the method lies in dividing the coil into a set of nested closed current loops of various sizes, with the magnetic field of each turn being calculated individually. At relatively low operating frequencies, where the length of the conductor comprising the planar spiral coil is much smaller than the wavelength at the operating frequency, it can be assumed that the current amplitude in the coil conductor is constant and uniform. This allows for the utilization of a quasi-static approximation of the magnetic field and subsequently calculating it using the Bio-Savart law, as follows:

$$\vec{B} = \frac{\mu_0 I}{4\pi} \oint \frac{[d\vec{r} \times (\vec{r_0} - \vec{r})]}{|\vec{r_0} - \vec{r}|^3}. \tag{1}$$

For a transmitting coil consisting of N turns, its total magnetic field is calculated as a superposition of magnetic fields created by each turn:

$$\vec{B} = \sum_{i=1}^{N} \vec{B}_i. \tag{2}$$

However, it is worth noting that the numerical solution of this integral is highly time-consuming and requires significant computational resources. To simplify the calculations, closed-form expressions for standard geometries can be utilized. For instance, the magnetic field of a current-carrying ring can be accurately calculated using closed equations containing complete and incomplete elliptic integrals [24]. The normal component of the magnetic field of each individual circular current loop to the plane of the coil can be calculated using the following equation:

$$B_z = \frac{\mu_0 I}{2\pi\alpha^2\beta}[(x_i^2 - r^2)E(k^2) + \alpha^2 K(k^2)], \tag{3}$$

where $r^2 = x^2 + y^2 + z^2$, $\alpha^2 = x_i^2 + r^2 - 2x_i\rho$, $\beta^2 = x_i^2 + r^2 + 2x_i\rho$, $\rho^2 = x^2 + y^2$, $k^2 = 1 - \alpha^2/\beta^2$, $K(k^2)$ is the complete elliptic integral of the first kind, and $E(k^2)$ is the incomplete elliptic integral of the second kind. Hereafter, equations for field calculations will be provided for the normal component of the magnetic field only, as this component primarily contributes to the power transfer efficiency in planar inductive WPT systems.

For spiral coils wound in a square, rectangular, or any other shape that can be represented as a piecewise-linear partition, the magnetic field of each individual turn is calculated as a superposition of fields from segments of current-carrying conductors. In this case, the normal component of the magnetic field to the plane of the segment with current connecting vertices of coordinates (x_1, y_1) and (x_2, y_2) is calculated as follows:

$$B_{z_i} = \frac{\mu_0 I}{4\pi} \cdot \frac{(x-\beta)\cdot\gamma}{\delta \cdot \sqrt{[\alpha\cdot(x-\beta)]^2 + \delta}}\Bigg|_{x_1}^{x_2}, \tag{4}$$

where $k = (y_2 - y_1)/(x_2 - x_1)$, $b = y_2 - kx_2$, $\alpha^2 = k^2 + 1$, $\beta = (x_0 + ky_0 - kb)/\alpha^2$, $\gamma = y_0 - (kx_0 + b)$, $\delta = {z_0}^2 + (\gamma/\alpha)^2$.

2.2. Encoding of Spiral Transmitting Coil for Optimization

In order to ensure the universality of the algorithm regardless of the transmitting coil shape, the distribution of turns is described using proportionality coefficients (PCs), and the coils themselves are defined, depending on their geometry, as follows: for a circular coil by the radius of the largest turn, for a rectangular coil by the length and width of the largest turn, and for a convex piecewise-linear coil by a list of the vertices' coordinates of the largest turn. Each turn in a multi-turn optimized coil is proportional to the largest possible turn by its respective PC; therefore, each PC identifies a specific turn size in the coil.

For the purposes of computer optimization using a GA, PCs are in turn encoded as bit arrays. The method presented in this paper allows for various degrees of discretization characterized by the discreteness parameter $\Delta = 1, 2, \ldots, M$, which defines how many bits are allocated for a single wire in the bit array, or, in other words, what portion of the $[0..1]$ segment of possible PC values is contained in one bit. It is recommended to pass an odd number to the Δ parameter. The length of the bit array l is defined as follows:

$$l = \Delta \cdot \left[\frac{1 - \mathrm{PC}_{\min}}{b \cdot d}\right], \tag{5}$$

where PC_{min} is the smallest possible PC, d the wire diameter, and b the bounds constant, a number that together with d characterizing the minimal distance between turns. b is calculated separately for circular, rectangular, and piecewise-linear geometries. The greater the Δ is, the longer the bit array is, which allows for more variety in the process of GA evolution in terms of possible values for PC, but requires computations that are more time consuming due to larger data structures.

Turn presence is defined by Δ consecutive "1" in the bit array. The central "1" in a sequence of length Δ at position $j = 1 \ldots l$ in the bit array defines the PC as follows:

$$PC = PC_{min} + \frac{(j-1)\cdot(1-PC_{min})}{l}. \quad (6)$$

2.3. Fitness Function for Transmitting Coil Optimization

In order to compare various transmitting coil geometries and subsequently optimize their magnetic field distributions, it is necessary to introduce a numerical assessment of the field uniformity. This can be achieved by using the coefficient of variation (COV), which is defined as the ratio of the root mean square deviation of the magnetic field intensity in the region of interest (ROI) to its mean value, calculated for N points in space where the magnetic field is measured.

$$COV_{B_z} = \frac{\sigma_{B_z}}{\mu_{B_z}} = \frac{\sqrt{\frac{1}{N-1}\sum_{k=1}^{N}\left(B_{zk} - \frac{1}{N}\sum_{k=1}^{N}B_{zk}\right)^2}}{\frac{1}{N}\sum_{k=1}^{N}B_{zk}}. \quad (7)$$

Thus, we obtain a dimensionless quantity characterizing the magnetic field uniformity in a specific region of the transmitting coil. A lower value of the COV indicates a more uniform magnetic field distribution.

2.4. Genetic Algorithm of Optimization

To obtain a rapid convergence rate, here we employ a GA for optimization task with large number of variables, namely PCs. We have used the conventional GA algorithm procedure. The optimization process begins with creating an initial random population consisting of individuals — variants of winding of a transmitting coil. In each iteration of the optimization cycle, the fitness function is calculated for each individual in the population, and the most "fit" individuals (those with a lower value of the fitness function) are selected for reproduction. The individuals undergo a crossover operation, and some individuals undergo random mutation before a new generation is created. These operations continue until the stopping criterion of reaching the maximum number of generations is met. Upon cycle termination, the individual with the minimum value of the fitness function is selected from the final generation. COV is used as the fitness function. PCs are the optimization variables, which correspond to the size of turns in the spiral coil, that are the arguments of the function for analytical field calculation. The hyperparameters of the GA, which is used further in this work, are summarized in Table 1. They were selected to ensure efficient and robust optimization process. The number of calculation points defines the discretization of the calculation domain, where the magnetic field of the spiral coil is calculated. It was selected to ensure a trade-off between computational efficiency and magnetic field calculation accuracy. The number of iterations was set to 50 based on preliminary tests showing convergence within 30–40 iterations, providing a margin for optimal results. The population size was chosen to balance computational efficiency and convergence speed, ensuring reasonable execution time. Other parameters were set according to standard GA practices to balance exploration and exploitation of the algorithm [25, 26].

TABLE 1. Genetic algorithm hyperparameters.

Parameter	Value
Population size	50
Number of iterations	50
Probability of mutation	0.1
Crossover probability	0.4
Calculation points	100
Tournament selection	4
Bit mutation	0.05

The software code implementing the described GA is written in the Python programming language using the DEAP (Distributed Evolutionary Algorithms in Python) library [27]. The standard cxMessyTwoPoint method is employed for crossover, the modified mutFlipBit method for mutation, and the eaSimple method for cyclical repetition of algorithm stages is used for optimization.

The input parameters of the GA include the coil shape, the size of the largest turn for circular and rectangular coils, a list of vertices' coordinates of the largest turn for piecewise-linear coil, and the size of ROI, where a uniform magnetic field distribution is required. The algorithm's output data include the number of coil turns and their PCs ensuring a minimum magnetic field variation. The average execution time of the proposed GA with the hyperparameters listed in Table 1 was around 40 seconds with a 10.8% CPU utilization (CPU: AMD Ryzen 7 5700U 1.80 GHz). The memory consumption during algorithm execution was measured at 123.5 MB.

3. RESULTS

3.1. Magnetic Field Analysis of Non-Optimized Transmitting Coils

First, we consider the magnetic field distribution of two basic transmitting coils: a single circular turn of radius r_{max}, shown in Fig. 1(a), and a spiral coil with an equidistant distribution of N turns from r_{min} to r_{max}, whose equivalent model is shown in Fig. 1(b). The magnetic field profiles at different relative heights above the considered coils calculated using (3) are presented in Fig. 1(c) and Fig. 1(d), respectively. Hereinafter, we will consider the field distribution at relative heights and in relative coordinates. When we go to absolute coil sizes and abso-

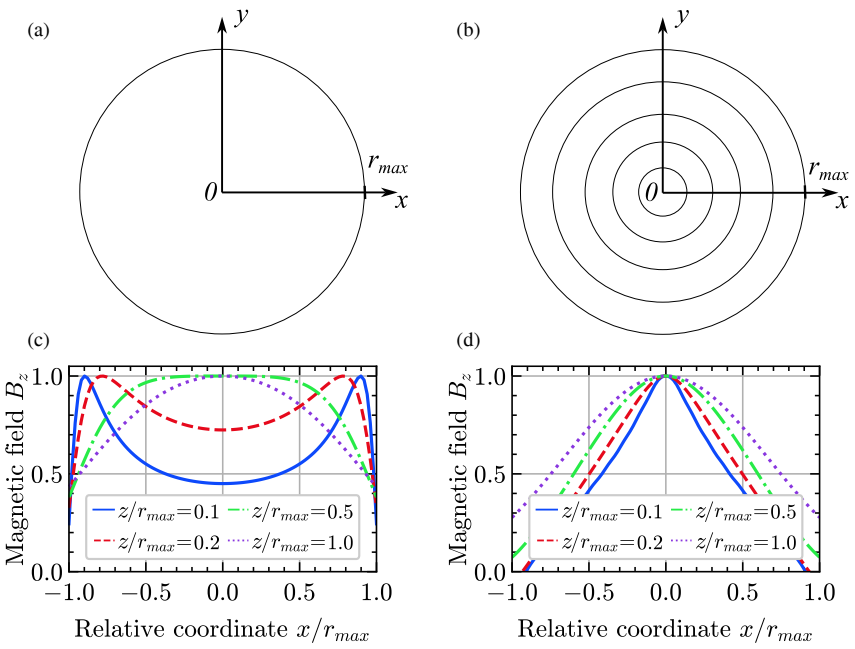

FIGURE 1. (a) Single turn coil and (c) its normalized magnetic field profile at different heights. (b) Equivalent model of multi-turn spiral coil and (d) its normalized magnetic field profile at different heights.

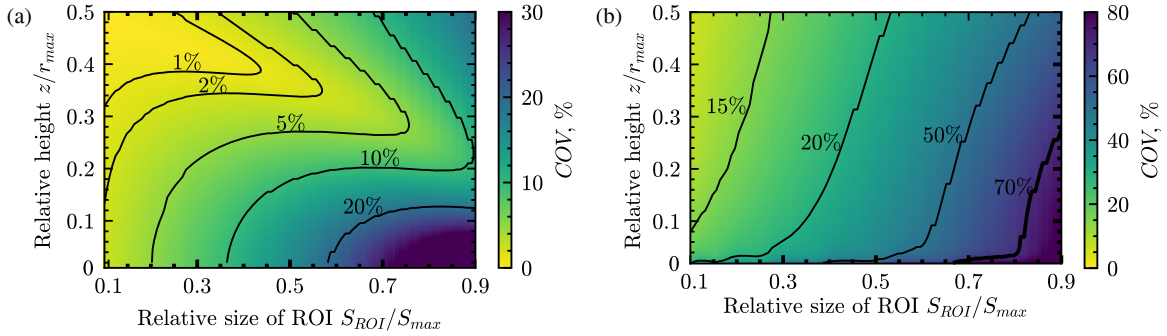

FIGURE 2. COV for different combinations of ROI size and height for (a) single-turn coil, (b) multi-turn coil.

lute ROI and target heights, the field distribution remains unchanged, and only its amplitude value changes.

From Fig. 1(c), one can see that the magnetic field profile of a single turn coil at low height $z/r_{\max} = 0.1$ has a concave shape — the field amplitude in the center of the coil is much smaller than its amplitude near the conductor. Moving away from the coil, the magnitude of the field tends to be more uniform. At the height of $z/r_{\max} = 0.5$ it becomes completely flat at the center, and the maximum field uniformity is achieved. At further distance from the coil, the field at the edges starts to decline, which also reduces the uniformity. The field distribution of an equidistant multi-turn coil has low uniformity regardless of height.

Obviously, the field uniformity in the ROI depends on its size. We calculate the COV of the field by (7) for both coils at different combinations of relative height and size of ROI. The resulting plots are shown in Fig. 2(a) for a single turn coil and in Fig. 2(b) for a multi-turn spiral coil. These plots also show that for a single coil there are combinations of height and ROI size for which high uniformity is achieved, but the relative heights for this purpose should be large and the size of the region of interest small, which makes the practical application of this type of transmitting coil impractical. For a multi-turn coil, high COV is observed for any combinations of height and ROI.

3.2. Optimization of Transmitting Coils

For practical usage of one-to-many WPT systems, it is necessary that the region with uniform field occupies an area of the transmitting coil as large as possible. In order to establish the minimum achievable COV values for planar spiral coils, a GA optimization of the coils is performed for each of the combinations of ROI size and height. Fig. 3 depicts the lowest achievable COV resulting from the optimization process. It is evident that the field uniformity of the optimized coils is markedly improved in comparison to that of the equidistant multi-turn coil (Fig. 2(b)) and even that of a single turn coil (Fig. 2(a)). The colormap demonstrates that through the optimization of the position and dimensions of the turns in planar spiral coils, a uniform field distribution in the vicinity of the coil can be achieved,

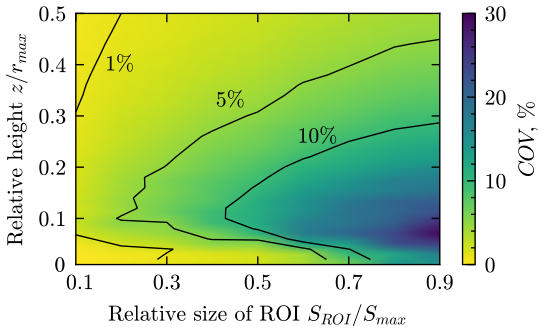

FIGURE 3. Minimal COV of multi-turn circular coil, optimized for different combinations of target height and ROI size.

which is of substantial importance for the practical implementation of one-to-many WPT systems.

To illustrate the convergence of the proposed algorithm, we shall consider the optimization of coils of circular, square, and hexagonal shapes, for different sizes of the computational domain. To this end, optimization process is conducted 50 times for each case, with the resulting COV values subjected to a statistical analysis. Fig. 4 illustrates the results of such an optimization. The height of the columns corresponds to the mean COV value, while the maximum and minimum COVs obtained from 50 optimizations are indicated by error bars. It can be observed that for ROI with relative size less than 0.5, the discrepancy between the optimization result and the mean is insignificant. Furthermore, under identical conditions, the COV of the magnetic field for circular coils is the lowest and for square coils is the highest. This is attributed to the fact that the magnetic field irregularities are formed in the corners of each coil.

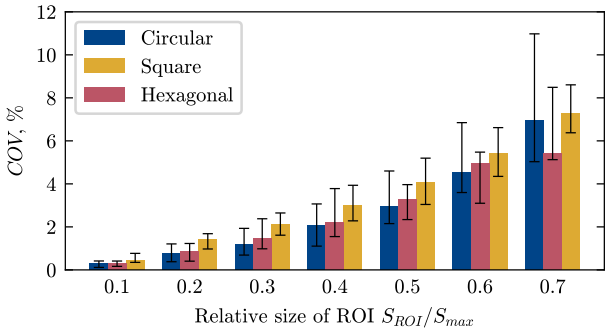

FIGURE 4. Results of multiple optimization of coils of different shapes at a fixed height of $z/r_{\max} = 0.24$. Bars show the mean value, error bars show the maximum and minimum COV from the dataset.

3.3. Fabrication of Coils and Experimental Verification of Optimization Results

To provide experimental confirmation of the results yielded by the proposed optimization GA, planar spiral coils of circular, square, and hexagonal shapes with an outer size of $r_{\max} = 12.5$ cm are fabricated. Optimized PCs for circular coil are: [0.208, 0.792, 0.84, 0.864, 0.888, 0.912, 0.936, 0.96, 0.984]; for square coil: [0.335, 0.757, 0.781, 0.814, 0.838, 0.862, 0.887, 0.911, 0.943]; for hexagonal coil: [0.128, 0.85, 0.878, 0.906, 0.934, 0.963]. Additionally, equidistant spiral coils are fabricated for experimental comparison of their magnetic field distributions with the optimized coils. The coils are implemented using Litz wire (28×0.1 mm) and placed in a mould, fabricated by 3D printing technology from PLA plastic. Fig. 6(a) and Fig. 6(c) illustrate the manufactured equidistant and optimized coils, respectively.

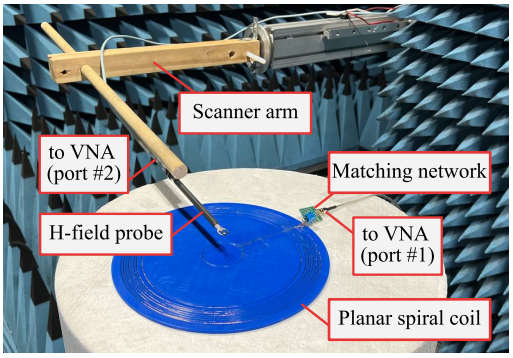

FIGURE 5. Photograph of the experimental setup for magnetic field measurements.

For each of the fabricated coils, the magnetic field distribution is measured. The photograph of the experimental setup is presented in Fig. 5. A planar S5048 vector network analyzer (VNA) is used for field measurement. The planar spiral coil is connected to one of the ports of the VNA through a resonant L-shaped matching circuit, which transformed the coil impedance to 50 ohms at a frequency of 200 kHz to increase the sensitivity of the magnetic field measurements. The nominal values of the L-shaped matching circuit elements for each coil were different, and they were calculated based on the measured inductance and resistance of each coil. A calibrated B-field probe Langer EMV XF-R 100-1 is connected to the second port of the VNA. The probe is positioned parallel to the planar spiral coil to detect the normal component B_z of the magnetic field only. The probe is mounted on a three-position scanner manipulator, which is used to scan the plane above the coil at a height of 30 mm with a 5 mm step. At each point, the transmission coefficient S_{21} between the planar spiral coil and magnetic field probe is measured using the VNA. The transmission coefficient is proportional to the intensity of the magnetic field created by the transmitting coil.

The measured distributions of the normalized magnetic field for all six fabricated transmitting coils are presented in Fig. 6(b) for the equidistant coils and Fig. 6(d) for the optimized ones. The COV is extracted from the measured magnetic fields using (7). The theoretical COV values are obtained from the field distributions, calculated by (3) and (4). Their comparison is illustrated in Fig. 7. A good agreement between analytical and experimental results is observed, confirming the accuracy of the mathematical model proposed in the paper. It can be observed that in the ROI with a relative size less than 0.5, it is possible to achieve COV less than 5% for each coil under test. Therefore, it can be concluded that the optimization algorithm allows for a significant increase in the homogeneity of the magnetic field distribution over the surface of the coils.

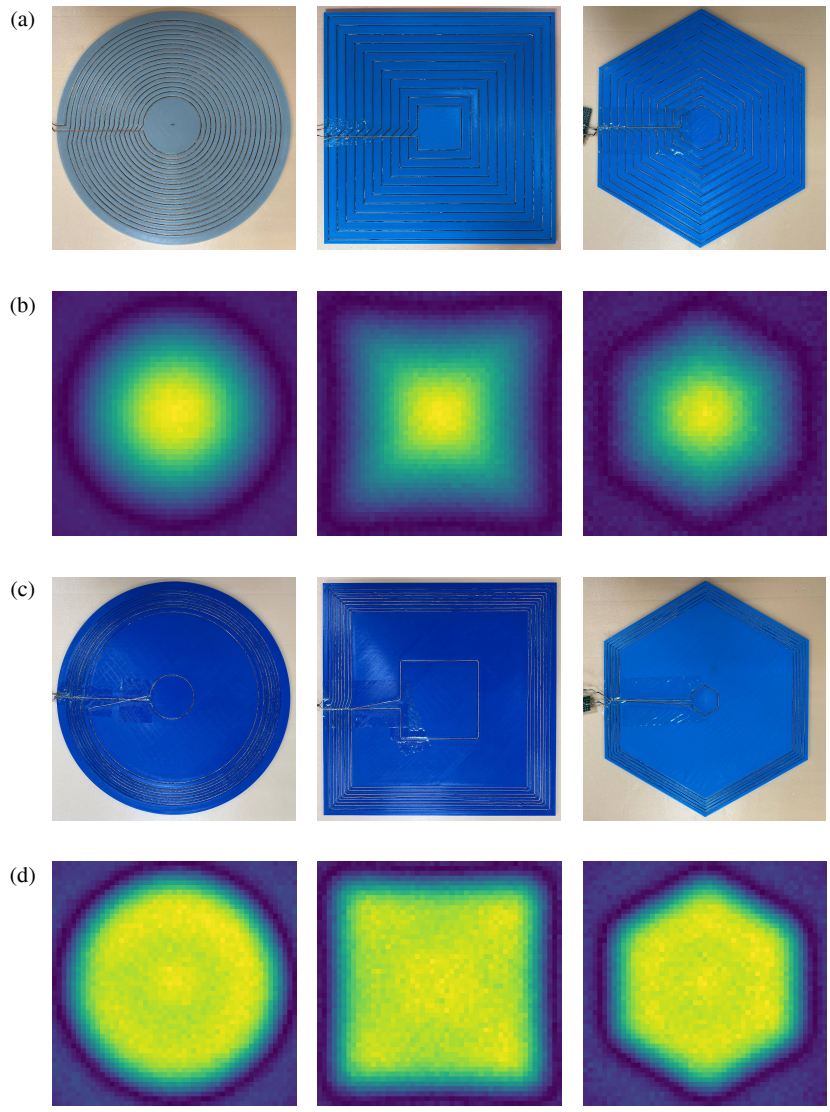

FIGURE 6. (a) Fabricated coils with equidistant winding, (b) measured normalized magnetic field distribution at 3 cm height of coils with equidistant winding, (c) fabricated optimized coils, (d) measured normalized magnetic field distribution at 3 cm height of optimized coils.

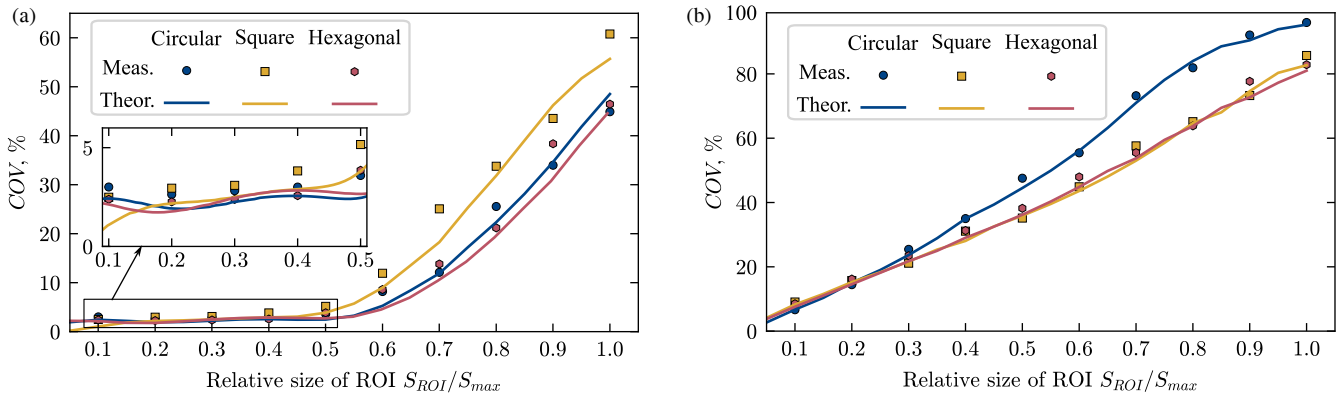

FIGURE 7. Comparison of calculated and measured COV of fabricated coils: (a) optimized coils, (b) equidistant coils. COV was calculated at the plane with 3 cm height (relative height $z/r_{\max} = 0.24$).

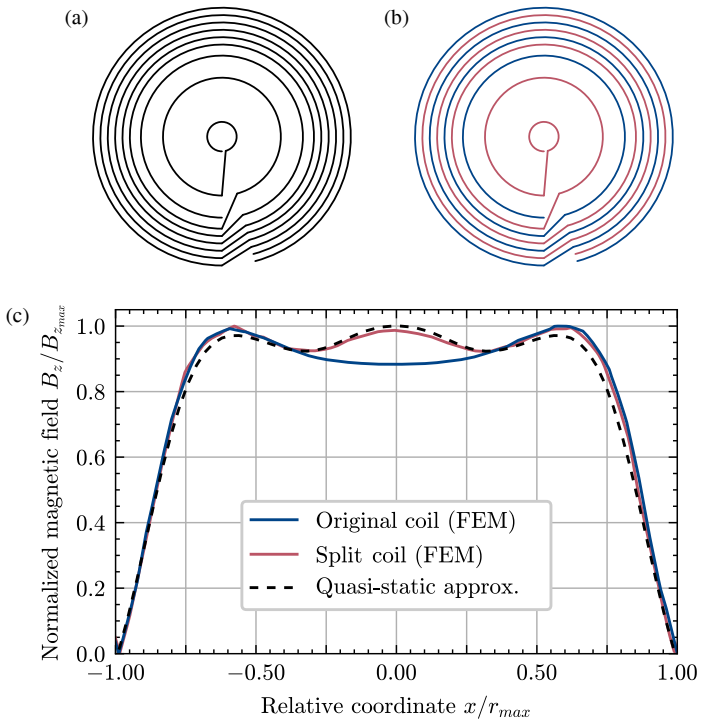

FIGURE 8. (a) Optimized multi-turn coil, (b) Multi-turn coil split into two coils (blue and red), (c) Normalized magnetic field distributions at 3 cm height obtained using quasi-static approximation and FEM simulation.

4. DISCUSSION

4.1. Optimization of Large-Scale Transmitting Coils

In developing the analytical model of a spiral coil in Section 2, we assume that the operating frequency of the system is sufficiently low, and the length of the conductor from which the coil is wound is much shorter than the wavelength at the operating frequency. These assumptions allowed us to utilize a quasi-static approximation and calculate the magnetic field of the coil according to the Biot-Savart law (1). However, in practice, there may arise situations where using a transmitter of significant size is necessary, meaning that the length of the winding conductor will be comparable to or even greater than the wavelength at the operating frequency, and reducing the system's operating frequency is not feasible. This could be due to various factors such as compliance with electromagnetic compatibility standards, high power requirements, safety considerations, etc. In such cases, applying a quasi-static approximation for the entire coil becomes impractical.

The solution to this problem could be dividing the spiral coil into multiple nested coils connected in parallel. The number of nested coils should be chosen such that the quasi-static approximation holds for each of them, meaning that the conductor's winding length is much smaller than the wavelength at the operating frequency. When developing an optimization algorithm for the transmitting coils, this constraint needs to be considered.

We have included this option in the proposed algorithm. For this purpose, the electrical length of the coil conductor is checked. If it is equal to or greater than the wavelength at the operating frequency of the WPT system, then the algorithm automatically suggests dividing a large transmitting coil into multiple nested ones. The division takes into account the resistance of the coil conductors so that equal currents flow through each coil when they are connected in parallel, ensuring that the magnetic field distribution aligns with the calculated values. This solution is realized by the greedy number partitioning algorithm and considers the resultant resistances of the obtained coils to minimize resistance differences between them.

To demonstrate this method, we considered the circular spiral coil presented in Section 3.3, with radius $r_{\max} = 12.5$ cm and optimized PCs [0.208, 0.792, 0.84, 0.864, 0.888, 0.912, 0.936, 0.96, 0.984] at 13.56 MHz operating frequency. In the case where it is wound from a single wire (shown in Fig. 8(a), its length becomes longer than the wavelength at the operating frequency. Fig. 8(c) shows the magnetic field distribution at a height of 3 cm above the coil (relative height $z/r_{\max} = 0.24$), numerically calculated using the finite element method (FEM) in the CST Studio Suite software. A discrete current source with an amplitude of 1 A was used as the power supply. It can be seen that there is a strong decrease of the magnetic field in the center and a discrepancy with the magnetic field distribution calculated by the quasi-static approximation. The calculated COV in ROI = $0.5S_{\max}$ for this case is 3.8%.

The coil was then split using the algorithm described above into two nested coils with the following PCs: [0.208, 0.792, 0.864, 0.912, 0.96] and [0.84, 0.888, 0.936, 0.984]. The conductor lengths for these coils are 2.93 m and 2.87 m, respectively. The resulting coils are shown in blue and red in Fig. 8(b). These coils were connected in parallel, and the resulting numer-

TABLE 2. Comparison of transmitting coils with uniform magnetic field distribution.

Ref.	Geometry	Coil size, cm^2/cm^3	Height, mm	Relative height z/r_{max}	Relative ROI size, S_{ROI}/S_{max}	COV, %	U, %
[21]	Square Planar	50×50	65	0.26	0.64	-	25
[28]	Rectangular 3D	$22 \times 18 \times 2$	0.5	0.005	0.30	-	20
[16]	Square Planar	20×20	50	0.5	0.52	-	18
[20]	Circular Planar	$10^2 \times \pi$	15	0.15	0.81	12.1	-
[29]	Rectangular 3D	$114 \times 28 \times 9$	30	0.05	0.68	-	10
[19]	Square Planar	80×80	100	0.25	0.42	-	9.6
[30]	Square Planar	50×50	18	0.072	0.49	-	7.2
[22]	Circular Planar	4.5×4.5	10	0.44	0.44	-	5
[14]	Square Planar	20×20	1	0.01	0.36	2.2	-
[31]	Square Planar	31.5×31.5	30	0.19	0.49	-	1
This paper	Circular Planar	$12.5^2 \times \pi$	30	0.24	0.50	3.6	7.6
This paper	Square Planar	25×25	30	0.24	0.50	5.2	13.8
This paper	Hexagonal Planar	25×21.7	30	0.24	0.50	5.1	8.5

ically calculated field distribution is shown in Fig. 8(c). A discrete current source with an amplitude of 2 A was used to power the split coil to ensure that the current in each coil was 1 A, as in the original coil. It can be seen that when the coils are split into two, the magnetic field distribution corresponds to that obtained using the quasi-static approximation. In this case, the COV in ROI = $0.5S_{max}$ is equal to 2.7%. Thus, we can conclude that dividing the coils into several nested coils connected in parallel allows us to preserve the field distribution calculated using the quasi-static approximation for large-scale transmitting coils.

It is also important to highlight the limitations of this segmentation approach. Given that the segmentation of the coil appears to be at the level of each single turn, this method appears applicable only to systems with the wavelength at the operation frequency much higher than the length of the largest turn. For systems operating at frequencies where the lengths of the largest turn approach a significant fraction of the wavelength, alternative transmitter design architectures such as multi-transmitter arrays [10] are recommended to maintain high field uniformity for misalignment tolerant and multi-load WPT systems.

4.2. Comparison with Other Transmitting Coils with Uniform Magnetic Field

Table 2 summarizes the main parameters of the transmitting coils with uniform magnetic field distributions, known from the literature. As all the works optimize coils of disparate sizes and at different target heights, in addition to the absolute values we provide relative ones. Some papers use an alternative uniformity parameter instead of COV, which is calculated as follows:

$$U = \frac{B_{max} - B_{min}}{B_{max}}. \tag{8}$$

Thus, the uniformity U, calculated for optimized coils by (8), is provided in Table 2 in addition to COV. Here, we note that the parameter U can also be used as a fitness function for the proposed algorithm. This option has been implemented in our algorithm, which is publicly available on GitHub [32]. However, the results of optimization using U as the fitness function are not included in the previous section to avoid overloading the text, as the resulting magnetic field distributions are nearly identical to those obtained using the COV. The distinction between these two metrics may become apparent during the evaluation of measured magnetic field distribution. Specifically, COV tends to average out measurement noise, which minimizes its impact on the results. In contrast, U is more sensitive to noise, as it directly compares the maximum and minimum field values at each measured point. In cases where the literature does not explicitly specify the ROI size or other key parameters, we estimate them by analyzing the provided field distribution plots.

As follows from the comparison, proposed circular coil has a slightly larger relative ROI with slightly lower uniformity U than [22]. At the same time, it has a significantly smaller COV than [20] but in smaller relative ROI size. Optimized square coil outperforms both designs reported in [28] and [16] in terms of uniformity U and relative ROI size, and outperforms [19] in terms of relative ROI size with comparable uniformity U. In [31] and [14], planar square coils have significantly lower uniformity and COV because they were calculated not from the field distribution, but from the voltage, induced on an Rx coil. The relative ROI size of 0.5, which was utilized for optimization in our work, can be considered a compromise value at which high magnetic field uniformity can be obtained. A larger relative ROI size can only be achieved by employing volumetric coils [28, 29] or by reducing the allowable field variation requirements [20].

The comparison of the primary features of the proposed optimization algorithm with other planar spiral coil optimization approaches recently reported in literature is summarized in Table 3. In contrast to prior methods that are limited to standard coil geometries (i.e., circular and rectangular), our algorithm provides a generalized framework capable of handling arbitrary convex polygonal coil shapes. In majority of the previously re-

TABLE 3. Comparison of the key features of the optimization algorithms of planar spiral coils with uniform magnetic field distribution.

Ref.	Arbitrary coil shape	Optimization of number of turns	Handling of large-scale coils	Open source
[21]	–	–	–	–
[16]	–	–	–	–
[20]	–	–	–	–
[29]	–	+	–	–
[19]	–	–	–	–
[30]	–	–	–	–
[14]	–	–	–	–
[31]	–	–	potentialy possible	–
This paper	+	+	+	+

ported approaches, the number of coil turns is predetermined, while the proposed algorithm optimizes it during the GA execution. A notable advantage of the proposed algorithm is its open-source availability [32], which facilitates extensive research and development. Additionally, we note the algorithm's ability to optimize large-scale coils for high-frequency applications due to the proposed segmentation approach.

5. CONCLUSION

This paper presents an analytical model for calculating the magnetic field of planar spiral coils of various shapes for the use in one-to-many WPT systems. An analysis of the magnetic field distribution was conducted on coils of a standard shape, namely a single coil and an equidistant multi-coil. A genetic algorithm was proposed for optimizing the distribution of coil winding in order to enhance the uniformity of the magnetic field within the specified region. The proposed algorithm is capable of optimizing not only standard transmitting coils, such as circular and square ones, but also convex polygonal coils. This capability is beneficial in the design of WPT coils that can be integrated into the casings of diverse products, thereby maximizing the available space and enhancing the performance of WPT systems. Validation of the algorithm via direct measurements of magnetic field distribution was carried out on three coils of distinct shapes: circle, rectangle, and hexagon. The outer dimensions of the coils were 25 cm, and the optimization was conducted for a relative ROI size of 0.5 at 30 mm height. The experimentally determined COV values at ROI were 3.6% for the circular, 5.2% for the square, and 5.1% for the hexagonal coils. The COV values obtained are superior to those reported previously in the literature. We provide open access to the developed software code that implements the proposed GA for spiral coils optimization for one-to-many WPT systems [32].

ACKNOWLEDGEMENT

This work was supported by the Russian Science Foundation under Project No. 23-19-00511, https://rscf.ru/project/23-19-00511/.

REFERENCES

[1] Song, M., P. Jayathurathnage, E. Zanganeh, M. Krasikova, P. Smirnov, P. Belov, P. Kapitanova, C. Simovski, S. Tretyakov, and A. Krasnok, "Wireless power transfer based on novel physical concepts," *Nature Electronics*, Vol. 4, No. 10, 707–716, Oct. 2021.

[2] Yu, X., J. Feng, L. Zhu, and Q. Li, "Design and optimization of a planar omnidirectional wireless power transfer system for consumer electronics," *IEEE Open Journal of Power Electronics*, Vol. 5, 311–322, 2024.

[3] Essa, A., E. Almajali, S. Mahmoud, R. E. Amaya, S. S. Alja'Afreh, and M. Ikram, "Wireless power transfer for implantable medical devices: Impact of implantable antennas on energy harvesting," *IEEE Open Journal of Antennas and Propagation*, Vol. 5, No. 3, 739–758, 2024.

[4] Moloudian, G., M. Hosseinifard, S. Kumar, R. B. V. B. Simorangkir, J. L. Buckley, C. Song, G. Fantoni, and B. O'Flynn, "RF energy harvesting techniques for battery-less wireless sensing, Industry 4.0, and Internet of Things: A review," *IEEE Sensors Journal*, Vol. 24, No. 5, 5732–5745, Mar. 2024.

[5] Ahmed, M. M., M. A. Enany, A. A. Shaier, H. M. Bawayan, and S. A. Hussien, "An extensive overview of inductive charging technologies for stationary and in-motion electric vehicles," *IEEE Access*, 69 875–69 894, 2024.

[6] Ramakrishnan, V., N. Rajamanickam, H. Kotb, A. Elrashidi, *et al.*, "A comprehensive review on efficiency enhancement of wireless charging system for the electric vehicles applications," *IEEE Access*, Vol. 12, 46 967–46 994, 2024.

[7] De Almeida, J. V., X. Gu, and K. Wu, "SWIPT base stations for battery-free, wirelessly powered IoT networks: A review on architectures, circuits and technologies," *IEEE Microwave Magazine*, Vol. 25, No. 6, 22–40, Jun. 2024.

[8] Zhong, W. X., X. Liu, and S. Y. R. Hui, "A novel single-layer winding array and receiver coil structure for contactless battery charging systems with free-positioning and localized charging features," *IEEE Transactions on Industrial Electronics*, Vol. 58, No. 9, 4136–4144, 2011.

[9] Zhang, C., W. Wang, C. Xu, and J. Yang, "Research on uniform magnetic field compensation structure of array circular coils for wireless power transfer," *IEEE Transactions on Magnetics*, Vol. 57, No. 6, 1–5, 2021.

[10] Jow, U.-M. and M. Ghovanloo, "Geometrical design of a scalable overlapping planar spiral coil array to generate a homoge-

neous magnetic field," *IEEE Transactions on Magnetics*, Vol. 49, No. 6, 2933–2945, Jun. 2013.

[11] Liu, X. and S. Y. Hui, "Optimal design of a hybrid winding structure for planar contactless battery charging platform," *IEEE Transactions on Power Electronics*, Vol. 23, No. 1, 455–463, 2008.

[12] Cai, C., J. Wang, H. Nie, P. Zhang, Z. Lin, and Y.-G. Zhou, "Effective-configuration WPT systems for drones charging area extension featuring quasi-uniform magnetic coupling," *IEEE Transactions on Transportation Electrification*, Vol. 6, No. 3, 920–934, 2020.

[13] Kudo, R., K. Hachiya, T. Kanamoto, and A. Kurokawa, "A bernoulli spiral coil transmitter for charging various small electronic devices," *IEICE Electronics Express*, Vol. 19, No. 23, 20 220 419–20 220 419, Dec. 2022.

[14] Casanova, J. J., Z. N. Low, J. Lin, and R. Tseng, "Transmitting coil achieving uniform magnetic field distribution for planar wireless power transfer system," in *2009 IEEE Radio and Wireless Symposium*, 530–533, San Diego, CA, USA, Jan. 2009.

[15] Kudo, R., K. Hachiya, T. Kanamoto, and A. Kurokawa, "A parabolic spiral coil transmitter with uniform magnetic field for smart devices," *IEICE Electronics Express*, Vol. 20, No. 1, 20 220 492–20 220 492, Jan. 2023.

[16] Wang, S., Z. Hu, C. Rong, C. Lu, J. Chen, and M. Liu, "Planar multiple-antiparallel square transmitter for position-insensitive wireless power transfer," *IEEE Antennas and Wireless Propagation Letters*, Vol. 17, No. 2, 188–192, Feb. 2018.

[17] Li, J., R. Qin, J. Sun, and D. Costinett, "Systematic design of a 100-W 6.78-MHz wireless charging station covering multiple devices and a large charging area," *IEEE Transactions on Power Electronics*, Vol. 37, No. 4, 4877–4889, Apr. 2022.

[18] Shen, L., W. Tang, H. Xiang, and W. Zhuang, "Uniform magnetic field by changing the current distribution on the planar coil for displacement-insensitive wireless power transfer/near field communication," *Microwave and Optical Technology Letters*, Vol. 57, No. 2, 424–427, Feb. 2015.

[19] Zhang, Y., L. Wang, Y. Guo, and Y. Zhang, "Optimisation of planar rectangular coil achieving uniform magnetic field distribution for EV wireless charging based on genetic algorithm," *IET Power Electronics*, Vol. 12, No. 10, 2706–2712, Aug. 2019.

[20] Xu, Q., Q. Hu, H. Wang, Z.-H. Mao, and M. Sun, "Optimal design of planar spiral coil for uniform magnetic field to wirelessly power position-free targets," *IEEE Transactions on Magnetics*, Vol. 57, No. 2, 1–9, Feb. 2021.

[21] Rong, C., X. He, Y. Wu, Y. Qi, R. Wang, Y. Sun, and M. Liu, "Optimization design of resonance coils with high misalignment tolerance for drone wireless charging based on genetic algorithm," *IEEE Transactions on Industry Applications*, Vol. 58, No. 1, 1242–1253, Jan.-Feb. 2022.

[22] Bilandžija, D., D. Vinko, and L. Filipović, "Genetic algorithm based optimization of circular planar coil geometry with homogeneous magnetic field distribution," in *2023 46th MIPRO ICT and Electronics Convention (MIPRO)*, 218–222, Opatija, Croatia, May 2023.

[23] Hui, S.-Y. R., Y. Yang, and C. Zhang, "Wireless power transfer: A paradigm shift for the next generation," *IEEE Journal of Emerging and Selected Topics in Power Electronics*, Vol. 11, No. 3, 2412–2427, Jun. 2023.

[24] Simpson, J. C., J. E. Lane, C. D. Immer, and R. C. Youngquist, "Simple analytic expressions for the magnetic field of a circular current loop," NASA, Tech. Rep., Feb. 2001.

[25] Kramer, O., *Genetic Algorithm Essentials*, Studies in Computational Intelligence. Springer Cham, 2017.

[26] De Rainville, F.-M., F.-A. Fortin, M.-A. Gardner, M. Parizeau, and C. Gagné, "DEAP: A python framework for evolutionary algorithms," in *Proceedings of the 14th Annual Conference Companion on Genetic and Evolutionary Computation*, 85–92, Philadelphia, PA, USA, Jul. 2012.

[27] Fortin, F.-A., F.-M. D. Rainville, M.-A. Gardner, M. Parizeau, and C. Gagné, "DEAP: Evolutionary algorithms made easy," *The Journal of Machine Learning Research*, Vol. 13, No. 1, 2171–2175, Jul. 2012.

[28] Lee, W.-S., H. L. Lee, K.-S. Oh, and J.-W. Yu, "Uniform magnetic field distribution of a spatially structured resonant coil for wireless power transfer," *Applied Physics Letters*, Vol. 100, No. 21, 214105, May 2012.

[29] Bilandžija, D., D. Vinko, and M. Barukčić, "Genetic-algorithm-based optimization of a 3D transmitting coil design with a homogeneous magnetic field distribution in a WPT system," *Energies*, Vol. 15, No. 4, 1381, Feb. 2022.

[30] Li, J., J. Sun, R. Qin, and D. Costinett, "Transmitter coil design for multi-load wireless power transfer systems," in *2020 IEEE Energy Conversion Congress and Exposition (ECCE)*, 1032–1038, Detroit, MI, USA, Oct. 2020.

[31] Zhang, C., W. Wang, C. Xu, and J. Yang, "Research on uniform magnetic field compensation structure of array circular coils for wireless power transfer," *IEEE Transactions on Magnetics*, Vol. 57, No. 6, 1–5, Jun. 2021.

[32] Miroshnikov, A., N. Zotov, P. Smirnov, and P. Kapitanova, "Spiral coil magnetic field optimizer," [Online]. Available: https://github.com/MiroshnikovAleksandr/Spiral-coil-magnetic-field-optimizer, 2024.